Pergamon

Tetrahedron 55 (1999) 1309–1320

TETRAHEDRON

The [1,4]Oxazino[4,3-*a*]azepine Ring System: Construction from Morpholinoallenes and a Structural Study

Gerhard Maas[a]*, Berthold Manz[b], Theo Mayer[b], and Udo Werz[a]

[a] Abteilung Organische Chemie I, Universität Ulm, Albert-Einstein-Allee 11, D-89081 Ulm, Germany
[b] Fachbereich Chemie der Universität Kaiserslautern, Erwin-Schrödinger-Straße, D-67663 Kaiserslautern, Germany

Received 23 October 1998; accepted 3 December 1998

Abstract: Morpholinoallenes **4** react with dimethyl and di(*tert*-butyl) acetylenedicarboxylate to form 4-alkylidene-3-morpholino-1-cyclobutenes **7** which undergo thermal rearrangement to [1,4]oxazino[4,3-*a*]azepine derivatives **8** and **9**. The structures of **7a**, **8aA**, and **8c** have been determined by single-crystal X-ray diffraction. A *cis*-fusion of the chair-like morpholine ring and the dihydroazepine ring is found in both **8aA** and **8c**, but the angular hydrogen atom is equatorial in **8aA** and axial in **8c**. NMR studies show that the respective chair conformation of the morpholine ring which is found in the solid state is also favored in solution, but temperature-variable spectra indicate that ring inversion is taking place.

Keywords: Allenes; azepines; bicyclic heterocyclic compounds; nitrogen heterocycles; conformation.

Introduction

It seems remarkable that N,N-dialkylaminoallenes, in which the electron-rich enamine function is combined with the [2]cumulene bond structure, have not yet found widespread use in organic synthesis. Previous investigations have revealed three potentially useful reactivity patterns: (a) Aminoallenes which bear a CH-substituent at either terminus of the allene function readily tautomerize by a hydrogen shift to form the corresponding 1- or 2-amino-1,3-dienes[1,2]. (b) (Dimethylamino)allene undergoes a smooth [2+2] cycloaddition reaction with electron-deficient alkenes[3] and alkynes[4]. The cycloadducts obtained with alkynes, 4-dimethylamino-3-methylenecyclobutenes **1**, rearrange thermally to 2,3-dihydroazepines **3** *via* 2-allenylenamines **2** (equation 1). (c) 3-Aryl- or 3-vinyl-1-(N-alkylamino)allenes can be isomerized thermally to dihydroazepine derivatives[5,6], e.g. **4** → **5** (equation 2).

If aminoallenes with the amino function incorporated in a ring sytem were submitted to the reaction sequence of equation 1, bicyclic azepine derivatives should be obtained that are structurally related to heterocycles **5**. We report now that the cycloaddition/isomerization sequence described for (dimethylamino)allene (equation 1) can be applied indeed to the highly substituted morpholinoallenes **4**. This procedure provides an access to novel 1,4-oxazino[4,3-*a*]azepine derivatives which are distinguished from **5** both by substitution pattern and functionalities.

* E-mail: gerhard.maas@chemie.uni-ulm.de

0040-4020/99/$ - see front matter
PII: S0040-4020(98)01132-6

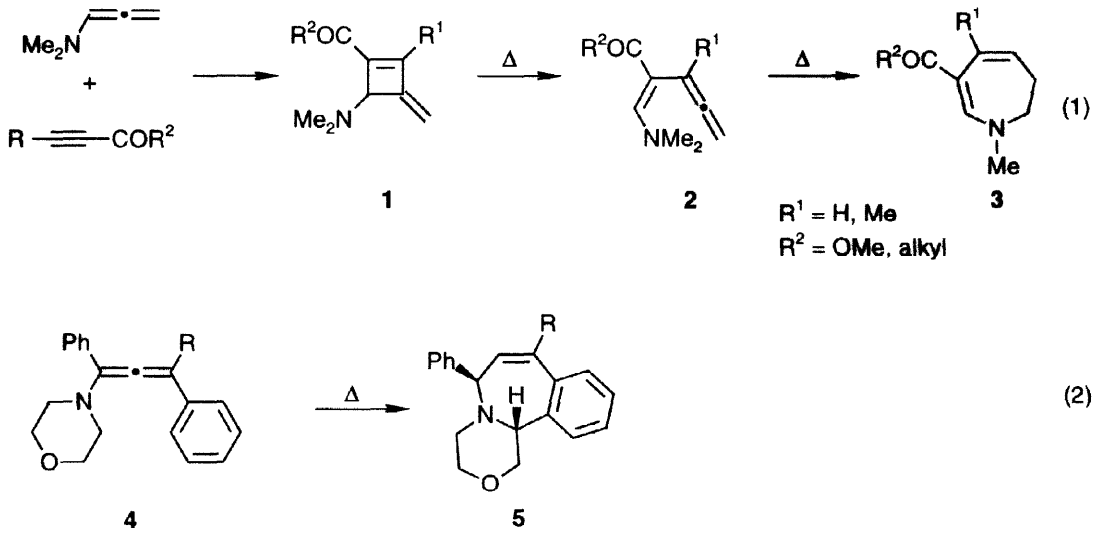

Results and Discussion

The reaction between equimolar amounts of morpholinoallene **4a** and dimethyl acetylenedicarboxylate (**6**) in ether was complete within one hour and yielded the formal [2+2] cycloaddition product **7a** as a mixture of diastereomers. The major isomer could be isolated by crystallization and was shown to have the *E*-configuration by single-crystal X-ray diffraction analysis (Figure 1). Thermal isomerization of **(*E*)-7a** took place upon heating in toluene (85 °C, 5 h), and the 1,4-oxazino[4,3-*a*]azepine derivative **8** was isolated in almost quantitative yield as a 3:2 mixture of diastereomers. Again, the major isomer could be isolated by fractionating crystallization and was identified by a crystal structure analysis as the *rel*-(10*S*,10a*R*) (or 10α,10aα) stereoisomer **8aA** (Figure 2). The *rel*-(10*R*,10a*R*) (or 10α,10aβ) configuration (**8aB**) was assigned to the second diastereomer based on the NMR spectra (vide infra). Complete isomerization of **(*E*)-7a** to **8a** occurred even at room temperature during several weeks (acetonitrile) or months (chloroform), whereas the crystalline cyclobutene remained unchanged during several months.

Similar to allene **4a**, morpholino(triphenyl)allene (**4b**) was transformed into bicyclic azepine derivative **8b**, and **4c** gave **8c** with dimethyl acetylenedicarboxylate and **9** with di(*tert*-butyl) acetylenedicarboxylate. In all three cases, the cycloaddition/isomerization sequence was carried out as a one-pot operation without isolation of the cyclobutene intermediate. Furthermore, it proved advantageous to use an excess (ca. 2 equivalents) of the liquid alkyne without an additional solvent. With this procedure, the intermolecular cycloaddition could be accelerated, and partial loss of the morpholinoallene by hydrolysis or slow thermal isomerization according to equation 2 could be suppressed. For comparison, reaction of **3b** with **6** by this procedure gave **8b** in a yield of 41 %, while equimolar amounts of the reactants in ether gave **5** (R = Ph, 15 %), **8b** (19 %) and ca. 8 % of dimethyl morpholinomaleate resulting probably from partial hydrolysis of the morpholinoallene.

In contrast to **8aA/B**, the replacement of a vinyl by a *tert*-butyl group resulted in the isolation of only one stereoisomer of **8c** and **9**. According to the single-crystal structure determination (Figure 3), the stereochemistry of **8c** is the same as for **8aA**, since the angular proton at C9 and the phenyl ring at C8 have a *syn*-relationship in both cases. However, the solid-state structures of **8aA** and **8c** are distinguished by two different ring conformations.

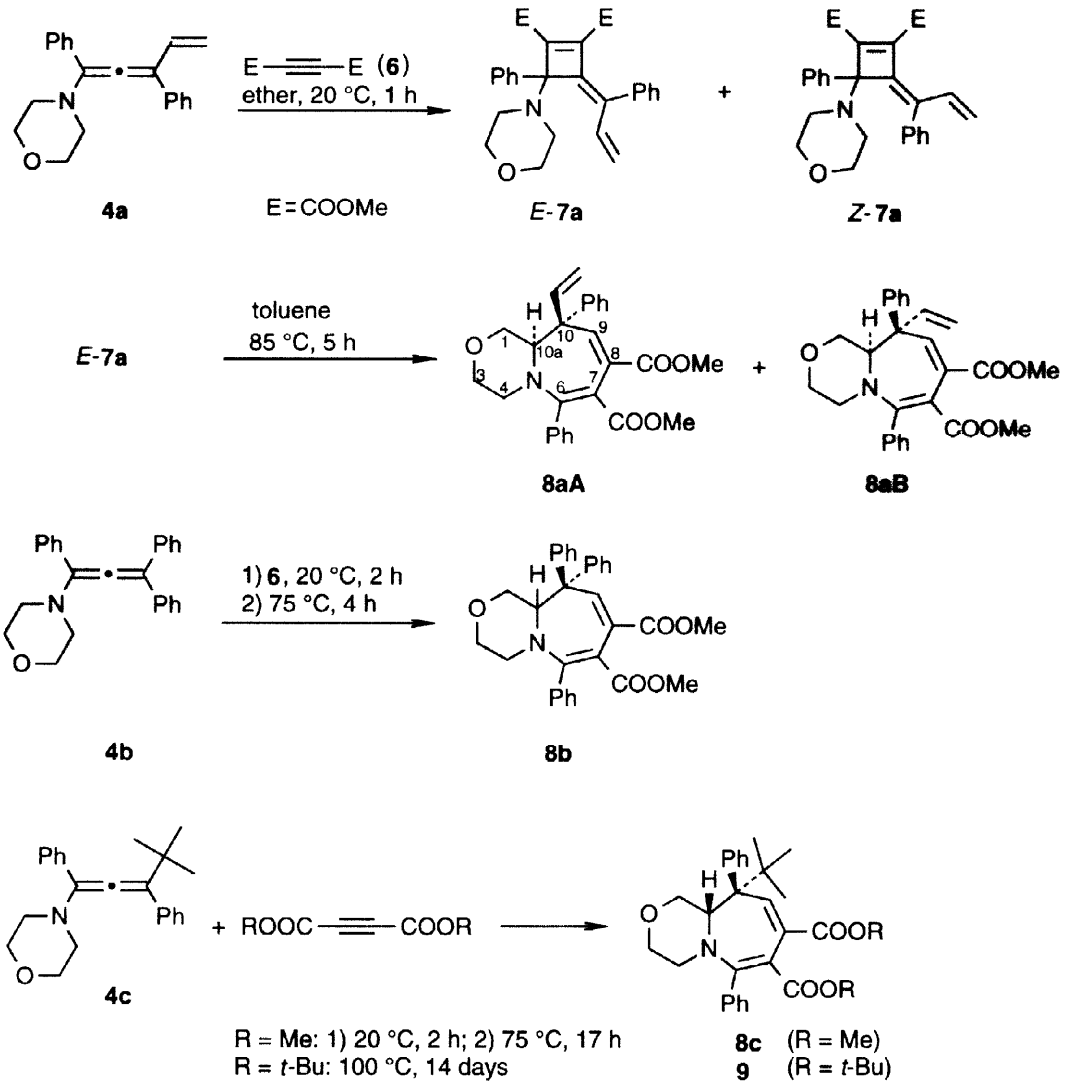

4a E-7a Z-7a

8aA 8aB

4b 8b

4c 8c (R = Me) 9 (R = t-Bu)

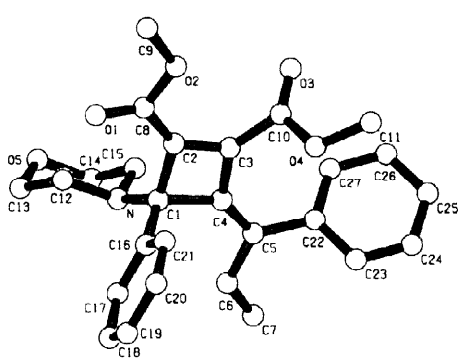

Figure 1. Structure of (*E*)-**7a** in the crystal (PLUTON plot). Selected bond lengths (Å): C1–C2 1.559(7); C1–C4 1.553(8); C2–C3 1.331(8); C3–C4 1.453(7); C4–C5 1.327(7); C2–C8 1.451(8); C3–C10 1.508(8). Bond angles (deg): C2–C1–C4 83.0(4); C1–C2–C3 92.7(4); C2–C3–C4 95.5(4); C3–C4–C1 88.5(4). Torsion angles (deg): C3–C2–C8–O1 167.7(6); C2–C3–C10–O3 69.5(9); C3–C4–C5–C6 179.2(6).

In mechanistic terms, it is suggested that the formation of the 1,4-oxazino[4,3-*a*]azepine ring system **8** from 4-alkylidene-3-morpholino-cyclobutenes **7** occurs in three steps. Initially, electrocyclic ring opening of **7** generates a (1,3,4-pentatrienyl)morpholine. In contrast to analogously formed 2-allenylenamines **2**[4], this compound could not be detected by NMR spectroscopy. A 1,6-hydride shift from a NCH_2 position to the

electron-deficient central allenic carbon atom generates a dipolar species which can be considered as an α,β,γ,δ-unsaturated azomethine ylide and which can undergo 1,7-cyclization[7] by a (conrotatory) 8π electrocyclic reaction. The H migration / electrocyclization sequence has been invoked to explain the thermal isomerization of a great variety of α,β,γ,δ-unsaturated amines, and the reactivity pattern is known under the names "*tert*-amino effect" [8,9] and "α-cyclization of teriary amines" [10].

*Structure and conformation of 1,4-oxazino[4,3-a]azepine systems **8** and **9***

*Crystal structure determination of **8aA** and **8c***. The structures of these two compounds in the solid state are shown in Figures 2 and 3; the arbitrary numbering scheme shown there is used for the discussion in this section. In both cases, the morpholine ring adopts a chair conformation, and the two rings are *cis*-fused. Nevertheless, two different conformations are found: While the attachment of the dihydroazepine ring to the morpholine ring in **8aA** is axial at C9 and pseudoequatorial at N, it is equatorial at C9 and pseudoaxial at N in **8c**. The nitrogen atom in **8aA** has a perfect trigonal-planar coordination but is still weakly pyramidalized in **8c** (sum of valence angles at N: 360.0 ° in **8aA** an 353.3 ° in **8c**). However, the expected bond length changes associated with π-conjugation in the enaminoester fragment (N–C4–C5–COOMe) are not very pronounced in both cases, most likely since the non-planarity of this moiety reduces the π-overlap. Corresponding torsion angles in the dihydroazepine rings of the two structures show large differences, which are attributed mainly to the different *cis*-fusion modes (see Newman projections along the N-C9 bond in Figures 2 and 3). The shape of the dihydroazepine ring in **8c** can be described approximately as an envelope conformation with C8 at the tip and C9 in between C8 and the major plane of the envelope. In **8aA**, the seven-membered ring can be considered to adopt an envelope form with C9 at the tip but deformed towards a boat-shaped structure with the N–C4 and C6–C8 bonds at the base and the C5–C6 bond displaced in the direction of C9. In both cases, the sterically more demanding substituent (Ph in **8aA** and *t*-Bu in **8c**) at C8 occupies the equatorial position at the seven-membered ring.

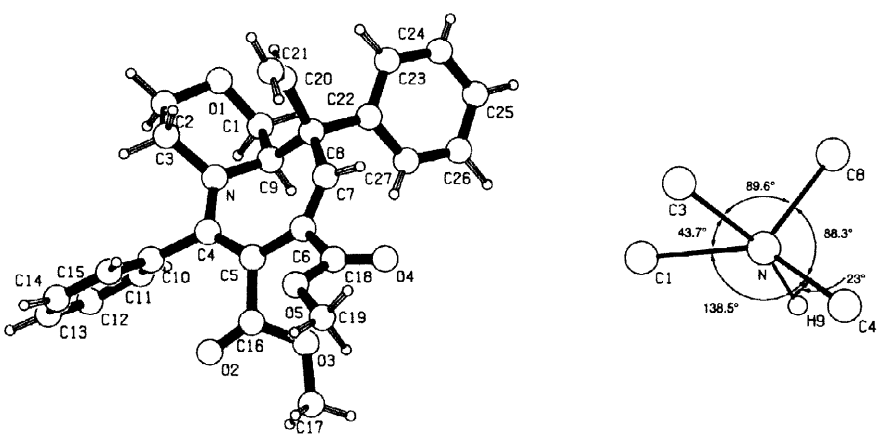

Figure 2. Structure of **8aA** in the crystal (PLUTON plot). Selected bond lengths (Å): N–C4 1.372(5); C4–C5 1.356(6); C5–C6 1.469(6); C5–C16 1.496(6); C6–C7 1.340(6); C6–C18 1.520(6). Bond angles (deg): C3–N–C9 118.2(4); C3–N–C4 121.2(4); C4–N–C9 120.5(5). Torsion angles (deg): C4–N–C3–C2 -138.6(4); C4–N–C9–C1 138.5(4); C4–N–C9–C8 -88.3(4); O1–C2–C3–N -50.4(5); O1–C1–C9–N 52.3(5); N–C4–C5–C6 21.4(7); C9–N–C4–C5 32.9(6); C4–C5–C16–O2 -30.5(7); C5–C6–C18–O4 143.2(5). A projection along the N–C9 bond and the torsion angles around this bond are shown on the right.

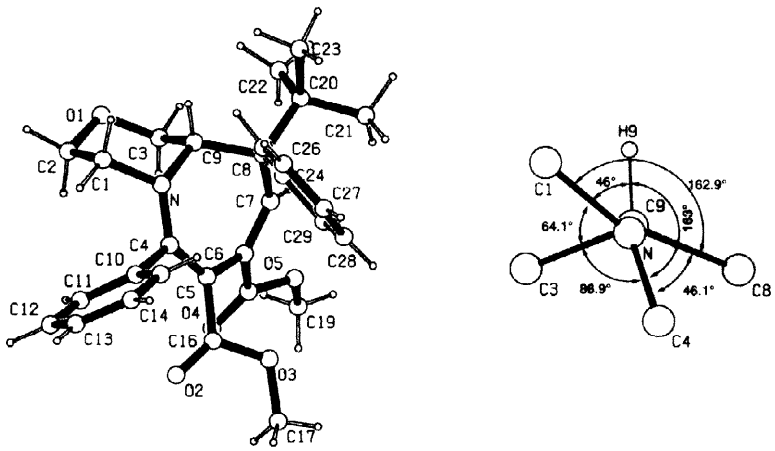

Figure 3. Structure of **8c** in the crystal (PLUTON plot). Selected bond lengths (Å): N–C4 1.389(5); C4–C5 1.365(5); C5–C6 1.475(5); C5–C16 1.476(6); C6–C7 1.330(5); C6–C18 1.497(6). Bond angles (deg): C1–N–C9 (108.3); C1–N–C4 120.2(3); C4–N–C9 124.8(3). Torsion angles (deg): C4–N–C1–C2 -90.8(4); C4–N–C9–C3 86.9(4); C4–N–C9–C8 -46.1(4); N–C1–C2–O1 -56.5(4); O1–C3–C9–N 62.6(4); N–C4–C5–C6 -4.6(6). C9–N–C4–C5 -1.3(5); C4–C5–C16–O2 34.7(6); C5–C6–C18–O4 21.7(5). A projection along the N–C9 bond and the torsion angles around this bond are shown on the right.

Conformation of 8 and 9 in solution. The solid state structures of **8aA** and **8c** indicate that the exchange of only one substituent at the position adjacent to the ring junction (*tert*-butyl vs. vinyl) is sufficient to realize the two possible modes of *cis*-fusion between the morpholine chair and the dihydroazepine ring. This observation led us to investigate whether the ring conformation in the solid state is also found in solution and whether chair/chair interconversion of the morpholine moiety would give rise to dynamic equilibria between structures **8-I** and **8-II** (**8a**: R^1 = Ph, R^2 = CH=CH_2; **8c**: R^1 = Ph, R^2 = *t*-Bu). Conformational equilibria of six-membered azaheterocycles with ring fusion at a C-N bond are rather common (see, for example, lit.[11-13]) and can result from ring inversion or N-inversion; in contrast to cases with sp^3-hybridized nitrogen, however, the latter process can be excluded in our cases since the nitrogen atom has a perfect (**8aA**) or approximate (**8c**) trigonal-planar coordination according to the crystal structure analyses presented above.

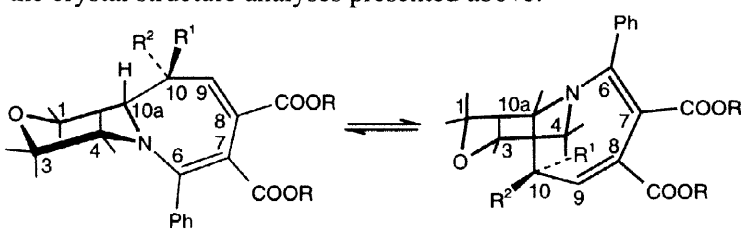

8-I **8-II**

For the conformational studies, ^{1}H and ^{13}C NMR spectra of **8a-c** and **9** were recorded at different temperatures. Signal assignments were extracted from 1D (selective TOCSY) spectra and 2D H,H and C,H correlation spectra. If needed, ^{13}C signals were also assigned based on long-range C,H correlation spectra (gradient-selected HMBC, optimized for 7 Hz couplings). Proton-proton coupling constants in the aliphatic region were taken from the 1D spectra directly. At 200 MHz, ^{1}H spectra of all compounds showed broadened signals at T ≈ 300 K due to dynamic exchange. While fast-exchange spectra could be obtained at 363 K ([D_8]toluene as solvent) for **8a-c** and at 304 K for **9**, cooling to 230-240 K was not sufficient to remove all signal broadening. Therefore, slow-exchange spectra of **8a-c** were recorded on a 500 MHz spectrometer at temperatures as low as necessary (Table 1), and the fast-exchange spectra were taken on a 200 MHz instrument at higher temperatures (Table 2). The ^{13}C NMR data obtained at low and high temperature are given in Table 3. Compound **9** showed a fast-exchange spectrum already at 304 K; since all signals were very broad even at 234 K, separate signal sets of the exchanging species could not be observed.

Table 1. ^{1}H NMR spectra (500 MHz, $CDCl_3$) of **8a-c** at temperatures of slow exchange (δ values [ppm], multiplicities, coupling constants [Hz] in parentheses)

Compound	Temp. [K]	1-H_{ax}	1-H_{eq}	3-H_{ax}	3-H_{eq}	4-H_{ax}	4-H_{eq}	10a-H	Other Signals
8aA	273	Isomer **8aA-I** (minor)							
		3.63[a]	4.07 d (11.2)	3.43[a]	3.70[a]	2.95–3.03 m		4.51 d (9.9)	3.26 (s, 3 H, OMe), 3.79 (s, 3 H, OMe), 5.21 (d, J = 10.7 Hz, 1 H, CH=CH_2), 5.26 (d, J = 17.3 Hz, 1 H, CH=CH_2), 5.92 (dd, J = 17.3, 10.7 Hz, CH=CH_2), 6.50 (d, J = 7.2 Hz, 1 H, o-H at 6-Ph), 7.20 (s, 1 H, 9-H), 7.25-7.48 (m, H_{arom})
		Isomer **8aA-II** (major)							
		3.64[a]	3.78[a]	3.52[a]	3.78[a]	2.91–2.96 m		3.79[a]	3.39 (s, 3 H, OMe), 3.75 (s, 3 H, OMe), 5.37 (d, J = 10.5 Hz, 1 H, CH=CH_2), 5.44 (d, J = 17.4 Hz, 1 H, CH=CH_2), 6.19 (s, 1 H, 9-H), 7.03 (dd, J = 17.4, 10.5 Hz, CH=CH_2), 7.25-7.56 (m, H_{arom})
8b	243	3.66 dd (10.5, 8.8)	3.97 d (10.5)	3.49 m_c	3.75 d[b] (11.5)	3.09–3.15 m		5.18 d (8.8[c])	3.35 (s, 3 H, OMe), 3.81 (s, 3 H, OMe), 6.49 (d, J = 7.4 Hz, 1 H, o-H at 6-Ph), 7.12-7.54 (m, 15 H, 9-H + 14 H_{arom})
8c	304	3.58–3.62 m[d]	4.20 d (10.0)	3.44 (11.6, 11.5,3.0)	3.58–3.62 m[d]	3.00 dt (11.6, 11.5,3.0)	3.09 dd (11.6, 2.6)	4.49 d (8.1[c])	1.03 (s, 9 H, CMe_3), 3.22 (s, 3 H, 8-OMe), 3.75 (s, 3 H, 7-OMe), 5.86 (d, J = 7.6 Hz, 1 H, o-H at 6-Ph), 7.07 (s, 1 H, 9-H), 7. 07-7.34 (m, 9 H, H_{arom})

[a] Due to overlap of signals of both conformers, coupling constants could not be determined. – [b] Doublet lines broadened due to further coupling (J < 2 Hz). – [c] ^3J(10a-H, 1-H^e) < 1 Hz. – [d] Signals of 1-H^a and 3-H^e overlap.

Table 2. ^{1}H NMR spectra (200 MHz) of **8a-c** and **9** at temperatures of rapid exchange (δ values [ppm], coupling constants [Hz])

Compound	Temp. Solvent	
8aA	363 K [D_8]toluene	δ = 2.59 (dd, J = 9.6, 4.2 Hz, 1 H, 4-H_1), 3.17 (s, 3 H, OMe), 3.10-3.27 (m, 3 H, 3-H_2, 4-H_1), 3.53 (s, 3 H, OMe), 3.48-3.64 (m, 2 H, 1-H_2), 3.80 (broad signal, 1 H, 10a-H), 5.04 (d, J = 10.6 Hz, 1 H, =CH_2), 5.24 (d, J = 17.5 Hz, 1 H, =CH_2), 6.63 (s, 1 H, 9-H), 6.99-7.92 (m, 11 H, H_{arom}, CH=CH_2)
8aB	363 K [D_8]toluene	δ = 2.28-2.39 (m, 1 H, 4-H_1), 2.78-3.73 (m, 5 H, 3-H_2, 1-H_2, 4-H_1), 3.20 and 3.61 (each s, 3 H, OMe), 3.87 (dd, J = 11.5, 5.2 Hz, 1 H, 10a-H), 5.10 (d, J = 10.6 Hz, 1H, =CH_2), 5.10 (d, J = 17.7 Hz, 1 H, =CH_2), 6.07 (dd, J = 17.7, 10.6 Hz, 1 H, CH=CH_2), 6.59 (s, 1 H, 9-H), 6.98-7.93 (m, H_{arom})
8b	363 K [D_8]toluene	δ = 2.54-2.60 (m, 2 H, 4-H_2), 3.06 (dd, J = 11.4, 6.4 Hz, 3-H_1), 3.10 (s, 3 H, OMe), 3.15 (dt, J = 11.1, 3.8 Hz, 3-H_1), 3.61 (s, 3 H, OMe), 3.71 (dd, J = 11.4, 7.9 Hz, 1 H, 1-H_1), 3.83 (dd, J = 11.4, 3.0 Hz, 1 H, 1-H_1), 4.74 (dd, J = 7.9, 3.0 Hz, 1 H, 10a-H), 6.89-7.44 (m, 16 H, 9-H, H_{arom})
8c	332 K [D_8]toluene	δ = 1.02 (s, 9 H, CMe_3), 2.57 (pseudo-t, 2 H, 4-H_2), 3.16 (s, 3 H, OMe), 3.20 (pseudo-t, 2 H, 3-H_2), 3.61 (s, OMe), 3.67 (dd, J = 11.7, 3.7 Hz, 1 H, 1-H_1), 3.91 (dd, J = 11.7, 7.5 Hz, 1 H, 1-H_1), 4.23 (dd, J = 7.5, 3.7 Hz, 1 H, 10a-H), 6.98-7.09 and 7.25-7.31 (m, 9 H, 9-H and H_{arom}), 7.60-7.65 (m, 2 H, H_{arom})
9	304 K $CDCl_3$ (500 MHz)	δ = 1.06 (s, 9 H, CMe_3), 1.09 (s, 9 H, CMe_3), 1.41 (s, 9 H, CMe_3), 2.75 (dd, J = 12.7, 2.6 Hz, 4-H_{eq}), 2.88 (ddd, J = 12.7, 11.5, 3.3 Hz, 4-H_{ax}), 3.33 (ddd, J = 11.5, 11.2, 2.6 Hz, 3-H_{ax}), 3.66 (dd, J = 11.2, 3.3 Hz, 3-H_{eq}), 3.73 (dd, J = 10.9, 10.9 Hz, 1-H_{ax}), 3.83 (dd, J = 10.9, 3.3 Hz, 10a-H), 3.93 (dd, J = 10.9, 3.3 Hz, 1-H_{eq}), 6.26 (s, 1 H, 9-H), 6.45 (br, 1 H), 6.92 (br, 1 H), 7.07 (br, 1 H), 7.14-7.30 (m, 7 H, H_{arom})

Table 3. ^{13}C NMR spectra of **8a-c** and **9** at different temperatures (δ {ppm}) [a]

Compound	Temp. Solvent	C-1	C-3	C-4	C-6	C-10	C-10a	Other Signals
8aA	243 K $CDCl_3$	Isomer **8aA-I** (minor)						
		70.91	67.51	53.54	157.19	50.55	71.11	50.76 (OMe), 52.32 (OMe), 100.10 (C-7), 114.89 (=CH_2), 126.13-137.85 (signals of both isomers), 126.43 (o-C at 6-Ph), 138.02 (C-9), 141.44, 142.14, 166.1 (7-C=O), 168.82 (8-C=O)
		Isomer **8aA-II** (major)						
		66.79	67.85	44.52	165.66	56.56	65.70	51.13 (OMe), 52.41 (OMe), 99.07 (C-7), 117.25 (=CH_2), 126.13-137.85 (signals of both isomers), 134.52 (C-9), 138.62 (*C*H=CH_2), 143.51, 168.80 (7-OMe), 171.58 (8-OMe)
	363 K [D_8]toluene	68.5	67.6	48.1*	159.7	56.0	68.5	50.4 (OMe), 51.7 (OMe), 103.7 (C-7), 116.3 (=CH_2), 125.0-130.3, 134.3, 136.2, 138.7, 141.0 (C-9), 144.1, 167.8 (C=O), 169.7 (C=O)
8aB	363 K [D_8]toluene	67.1	66.8	46.3	160.1	56.0	68.5	50.5 (OMe), 51.7 (OMe), 103.4 (C-7), 116.7 (=CH_2), 125.0-130.3, 134.2, 136.7, 138.7, 141.7 (C-9), 141.8, 168.4 (C=O), 170.2 (C=O)
8b	243 K $CDCl_3$	70.91	67.42	53.91	157.42	52.15	70.42	50.94 (OMe), 52.42 (OMe), 99.35 (C-7), 126.03-130.33 (8 signals), 126.43 (o-C at 6-Ph), 135.23, 137.64, 140.82 (C-9), 142.85, 143.89, 166.34 (C=O), 168.89 (C=O)
	363 K [D_8]toluene	69.9	67.5	51.7	157.6	55.6	70.0	50.3 (OMe), 51.7 (OMe), 103.7 (C-7), 125.0-129.8, 135.6, 139.1, 139.7 (C-9), 144.5, 144.9, 167.0 (C=O), 169.0 (C=O)
8c	304 K $CDCl_3$	71.82	67.59	55.25	154.36	55.88	67.37	28.52 (CMe_3), 37.18 (*C*Me_3), 50.71 (OMe), 52.08 (OMe), 102.38 (C-7), 125.41-131.17 (8 signals), 126.78 (o-C at 6-Ph), 134.96 (C-8), 137.14 (C-9), 138.62, 139.84, 166.99 (C=O), 169.16 (C=O)
	333 K [D_8]toluene	68.5	67.2	50.1*	157.8*	58.4	68.7	28.6 (CMe_3), 40.1 (*C*Me_3), 50.5 (OMe), 51.8 (OMe), 106.1* (C-7), 124.9-130.4, 133.7, 138.6, 138.9, 141.3, 168.1 (C=O), 170.2 (C=O)
9	333 K [D_8]toluene	68.1	66.9	45.4	158.9	59.1	68.2	28.1 (CMe_3), 28.4 (CMe_3), 30.5 (*C*Me_3), 37.6 (*C*Me_3), 77.3 (O*C*Me_3), 80.0 (O*C*Me_3), 106.2 (C-7), 121.3 (C-9), 124.9-130.2, 133.1, 139.9, 150.1, 163.9 (C=O), 172.3 (C=O).

[a] Spectra in $CDCl_3$ were taken at 125.77 MHz, spectra in [D_8]toluene at 100.6 MHz. Signals marked with "*" are broad due to coalescence.

The vicinal H,H coupling constants of the angular proton 10a-H characterize the type of *cis*-fusion at the chair-like morpholine ring. If this proton is in the axial position as in **8-I**, large diaxial coupling (ca. 8-11 Hz) with 1-H_{ax} is expected as compared to very small axial-equatorial coupling with 1-H_{eq}. If 10a-H occupies the equatorial position as in **8-II**, two intermediate coupling constants to the protons at C-1 are predicted based on dihedral angles of about 60 °. As far as coupling constants in the NCH_2-CH_2O part of the molecules can be determined, one finds a large (axial-axial) and a small (axial-equatorial) vicinal coupling constant, in line with a staggered conformation. In detail, the following observations were made for **8a-c** and **9**.

The ^{1}H NMR spectrum (500 MHz) of **8aA** shows signals for two species at T = 233 and 273 K. A dynamic equilibrium is indicated by temperature-dependent ratios (27:73 at 233 K and 37:63 at 273 K) and by coalescence of all signals at 303 K. The fast-exchange spectrum of **8aA** was recorded at 363 K in [D_8]toluene. The two sets of signals observed in the low-temperature spectra are assigned to conformers **8aA-I** and **8aA-II** (R^1 = Ph, R^2 = CH=CH_2). For the minor component (**8aA-I**), the axial position of the angular proton H-10a at the morpholine chair is indicated by a doublet signal at δ = 4.51 ppm with ^3J = 9.9 Hz. Moreover, this conformer shows a signal at 6.50 ppm which was assigned unambiguously to one of the ortho protons of the phenyl ring at C-6. Obviously, this phenyl ring is perpendicular to the N-C=C plane and does not rotate freely. In this position, one of the ortho protons experiences magnetic shielding by the phenyl ring attached to C-10. While this arrangement corresponds exactly to the solid state structure of **8c** (Figure 3), the major component in the conformational equilibrium should have the structure **8aA-II** which was also found for crystalline **8aA** (Figure 2). The salient differences of its ^{1}H NMR spectrum to that of **8aA-I** are the following: No signal for an aromatic proton at unusually high field is observed, the resonance of the olefinic proton 9-H appears at 6.19 ppm (i.e. upfield by 1.01 ppm compared to the other conformer), and the morpholine protons resonate at δ ≤ 3.79 ppm. The signal of 10a-H could be localized by 2D techniques at δ = 3.79 ppm which corresponds to an upfield shift of 0.72 ppm with respect to the axial proton 10a-H in **8aA-I**. Unfortunately, overlap with other signals of both conformers does not allow reliable determination of the coupling constants for this proton. However, an inverse H,C correlation spectrum (HMQC) shows a cross peak which is not split by H,H spin coupling, i.e. J(H,H) < 4.5 Hz, as one would expect for the equatorial position of this proton at the morpholine chair. Characteristic differences between the two conformers are also found in their ^{13}C NMR spectra. In particular, one notes high-field shifts for C-1, C-4, C-10a in the major conformer **8aA-II**, and for C-6, C-10 in **8aA-I**. The shieldings are likely to result from various γ-effects in which not only ring atoms but also carbon atoms attached to the azepine ring can be involved.

Compound **8aB** is the C-10 epimer of **8aA**. Since it could not be obtained in analytically pure form, its dynamic behavior has not been studied. The close similarity of the ^{13}C chemical shifts at T = 363 K indicates that the conformers in equilibrium are very similar in both cases. In the time-averaged ^{1}H NMR spectrum, the observation of a large ^3J coupling (11.5 Hz) for 10a-H suggests that the dominating conformer has this proton in an axial position at the morpholine chair.

Compounds **8b** and **8c** are rather similar with respect to their conformation and dynamic behavior. In both cases, the slow-exchange spectra (^{1}H and ^{13}C) show the presence of only one conformer. The characteristic features of the spectra parallel those of **8aA-I** (see above) and are in harmony with the solid-state structure of **8c**. The 500 MHz ^{1}H NMR spectrum of **8b** is static at 243 and 273 K, while line-broadening of most signals is observed at 303 K. The fact that the signals of NCH, NCH_2, and 6-Ph have become particularly broad indicates that the acceleration of chair/chair interconversion and of the rotation of 6-Ph is responsible for the coalescence phenomena. In the 200 MHz ^{1}H NMR spectra of **8b** (solvent: [D_8]toluene), line broadening sets in already above 248 K, and most signals appear as sharp lines again at 363 K. The hindered rotation of 6-Ph no longer exists, and the chemicals shifts of the morpholine protons have changed by only 0.3 ppm or less. The signal of 10a-H has changed from a doublet [at 248 K: δ = 4.84 ppm, ^3J = 8.6 Hz] to a doublet of doublets [δ = 4.74 ppm, ^3J = 7.9 and 3.0 Hz]. Analogously, the ^{13}C NMR spectrum of **8b** at low temperature resembles closely (with respect to the comparable signals) to that of **8aA-I**, while the high-temperature spectrum reveals similar changes for the chemical shifts of the ring carbon atoms as in the case of the equilibrium **8aA-I/8aA-II**. Taking together all observations, it appears that **8b** exists at all temperatures largely in the form **8b-I**, for which rotation of the phenyl ring attached to C-6 is slow on the NMR time scale at low temperature. When the temperature is raised,

8b-I equilibrates with only minor amounts of conformer **8b-II** due to morpholine ring inversion, and the phenyl ring at C-6 can rotate freely.

The 500 MHz ^{1}H spectrum of **8c** in [D_8]toluene was recorded at 227, 304, and 363 K. While no dynamic exchange is seen at the low temperature, line-broadening occurs at 304 K in the aromatic region only, due to accelerated rotation of the phenyl ring at C-6, but not for the morpholine signals. The latter retain their coupling pattern over the whole temperature range, while the chemical shifts are somewhat temperature-dependent. A spectrum taken from a $CDCl_3$ solution does not yet show line-broadening at 304 K (Table 1). In the 200 MHz ^{1}H spectra ([D_8]toluene), almost all signals are affected by coalescence processes at T = 228 K, line-broadening for the morpholine protons is still present at 296 K, and a time-averaged spectrum with sharp lines is obtained at 332 K. These observations suggest again that **8c** exists mainly in the form **8c-I**; furthermore, the temperature-dependent 500 MHz spectra seem to indicate that the acceleration of the rotation of 6-Ph is not coupled with a major conformational change of the bicyclic ring system.

Compounds **8c** and **9** differ only by the nature of the ester groups. However, the presence of COO*t*-Bu rather than COOMe substituents at C-7 and C-8 strongly lowers the temperature for NMR observation of dynamic processes. Already at 234 K, all signals of the 500 MHz ^{1}H NMR spectrum are either broadened or in coalescence. At 304 K, the signals of the morpholine and *t*-Bu protons have sharp lines again, but residual line-broadening is observed for some of the aromatic protons (Table 2). The latter spectrum shows H,H coupling constants for the morpholine protons at C-1, C-3, and C-4 which are very similar to those of **8c** in the slow-exchange spectrum (Table 1). This raises the question about the nature of the dynamic process observed for **9**. Eventually, it is simply a conformational change which affects mostly some ring atoms and substituents of the seven-membered ring but does not entail a chair/chair interconversion of the morpholine ring. This issue could not be clarified since our instrumental device did not allow to record spectra below 220 K in order to identify the exchanging species.

In summary, we have shown that the conformation of the bicyclic ring system present in **8** and **9** is very sensitive to the nature of substituents at the seven-membered ring. Since crystal structure analyses of **8aA** and **8c** reveal the trigonal-planar coordination around the nitrogen atom at the ring fusion, N-inversion can be excluded as the source of the conformational equilibria observed in solution. Rather, chair/chair interconversion of the morpholine ring occurs in **8a-c**. In the case of **9**, which bears two neighboring, sterically demanding COO*t*Bu groups at the seven-membered ring, a conformational change involving mostly some atoms and substitutents of this ring could be the most facile dynamic process observed on the NMR time scale.

Experimental

General Information. All reactions were carried out in rigorously dried glassware and under an argon atmosphere. Solvents were dried by standard procedures and kept under argon. For preparative column chromatography, silica gel (0.063–0.2 mm) from Macherey & Nagel was applied; the petroleum ether used for eluation had a boiling point of 40-60 °C. Melting points were determined in a copper block. – NMR spectra: Bruker WP 200 (^{1}H: 200.1 MHz), Bruker AMX 400 (^{1}H: 400.1 MHz; ^{13}C: 100.6 MHz), and Bruker AMX 500 (^{1}H: 500.14 MHz; ^{13}C: 125.77 MHz). All spectra were recorded in $CDCl_3$ solution, if not stated otherwise. As internal standard, TMS was used for ^{1}H spectra, and the solvent signal for the ^{13}C spectra [$\delta(CDCl_3)$ = 77.0, $\delta(C_6D_5\text{-}CD_3)$ = 20.4 ppm]. – IR spectra: Perkin-Elmer 1310 Infrared Spectrophotometer; wavenumbers [cm^{-1}] are given. – Elemental analyses: Perkin-Elmer EA 2400.

Dimethyl 3-Morpholino-3-phenyl-4-[(*E*)-(1-phenyl-2-propenylidene]-1-cyclobutene-1,2-dicarboxylate (7a): The solution of **4a**[1] (640 mg, 2.10 mmol) and of dimethyl acetylenedicarboxylate (**6**) (300 mg, 2.10 mmol) in diethylether (35 mL) was stirred for 60 min. After concentration to a volume of 10 ml and addition of pentane, a red, crystalline diastereomeric mixture of ***E***- and ***Z*-7a** was obtained (460 mg, 49 %, *E*/*Z* = 5.0). Recrystallization from dichloromethane–ether (1:3) furnished pure ***E*-7a** as pale-yellow crystals, mp 130 °C. – IR (KBr): ν = 1750 (s, C=O), 1720 (s, C=O), 1650 (m), 1570 (m), 1440 (s), 1250 (s) 998 (s) cm^{-1}. – ^{1}H NMR ($CDCl_3$, 400 MHz): δ = 2.82-2.91 (m, 4 H, NCH_2), 3.26 (s, 3 H, OMe), 3.73-3.81 (m, 4 H, OCH_2), 3.74 (s, 3 H, OMe), 4.95 (dd, *J* = 17.3, 1.2 Hz, 1 H, =CH_2-trans), 5.30 (ddd, *J* = 10.6 and 1.2 Hz, 1 H, =CH_2-cis), 7.03-7.70 (m, 11 H, C*H*=CH_2 and H_{arom}). – ^{13}C NMR ($CDCl_3$): δ = 48.6 (NCH_2), 51.7 (OMe), 52.0 (OMe), 67.5 (OCH_2),

80.7 (C-3), 120.6 (=CH_2), 128.4-129.8 (*o*-, *m*-, *p*-C_{arom}), 133.8 (=CH_{vinyl}), 134.0 (*i*-C_{arom}), 135.5 (=*C*(Ph, vinyl)), 138.6 (*i*-C_{arom}), 140.5, 141.6 (C-1 and C-2), 150.1 (C-4), 161.9 (C=O). – Anal. calcd. for $C_{27}H_{27}NO_5$ (445.5): C, 72.79; H, 6.11; N, 3.14. Found: C, 72.0; H, 6.0; N, 3.0.

Isomer **Z-7a** was not isolated in pure form; it was identified by the following ^{13}C NMR signals in the crude *E/Z* mixture: δ = 48.6 (NCH_2), 51.2 (OMe), 51.5 (OMe), 66.3 (OCH_2), 81.3 (C-3), 119.6 (=CH_2), 147.6 (C-4).

Dimethyl 6,10-Diphenyl-10-vinyl-3,4,10,10a-tetrahydro-1*H*-[1,4]oxazino[4,3-*a*]azepine-7,8-dicarboxylate (8a): A solution of **(*E*)-7a** (140 mg, 0.31 mmol) in toluene (30 mL) was heated at 85 °C during 5 h. The solvent was evaporated, and the residue was crystallized from pentane to give a yellow powder which was a diastereomeric mixture of **8a** (130 mg, 93 %, (*rel*-10*S*,10a*R*):(*rel*-10*R*,10a*R*) = 3:2). The major diastereomer (**8aA**) could be obtained in pure form by recrystallization from ether–pentane (4:1) followed by recrystallization from ethyl acetate as colorless crystals, mp 144 °C; yield: 40 mg (29 %). The minor diastereomer (**8aB**) was obtained from the combined mother liquors but could not be purified completely. – Spectroscopic and analytical data for the *rel*-(10*S*,10a*R*)-isomer (**8aA**): IR (KBr): ν = 1718 (s), 1530 (m), 1415 (w), 1235 (s), 1225 (s), 1095 (s) cm^{-1}. – ^1H NMR: Tables 1 and 2. – ^{13}C NMR: Table 3. – Anal. calcd. for $C_{27}H_{27}NO_5$ (445.5): C, 72.79; H, 6.11; N, 3.14. Found: C, 72.0; H, 6.3; N, 3.1.

Dimethyl 6,10,10-Triphenyl-3,4,10,10a-tetrahydro-1*H*-[1,4]oxazino[4,3-*a*]azepine-7,8-dicarboxylate (8b): Allene **4b**[1] (621 mg, 1.78 mmol) was combined with dimethyl acetylenedicarboxylate (**6**) (0.43 mL, 3.51 mmol), and the resulting deep-brown solution was stirred at 20 °C for 2 h, then at 75 °C for 4 h. Ether was added, and after filtration over a pad (ca. 5 g) of silica gel, the volatiles were evaporated, and the residue was recrystallized from acetonitrile. Colorless crystals of **8b** were obtained, mp 176 °C; yield: 355 mg (41 %). – IR (KBr): ν = 1717 (s), 1545 (m), 1480 (w), 1430 (m), 1265 (m), 1110 (s), 1090 (m) cm^{-1}. – ^1H NMR: Tables 1 and 2. – ^{13}C NMR: Table 3. – Anal. calcd. for $C_{31}H_{29}NO_5$ (495.6): C, 75.13; H, 5.90; N, 2.83. Found: C, 74.8; H, 5.9; N, 2.8.

Dimethyl *rel*-(10*S*,10a*S*)-10-(*tert*-Butyl)-6,10-diphenyl-3,4,10,10a-tetrahydro-1*H*-[1,4]oxazino[4,3-*a*]azepine-7,8-dicarboxylate (8c): Allene **4c**[1] (250 mg, 0.75 mmol) and dimethyl acetylenedicarboxylate (**6**) (0.2 ml, 1.22 mmol) were combined, and the resulting deep-brown solution was stirred at 20 °C for 2 h, then at 75 °C for 7 h. After evaporation (0.001 mbar) of excess alkyne, the residue was dissolved in ether-petroleum ether (1:1) and filtered over a pad of silica gel (ca. 5 g). The product was then recrystallized from acetonitrile to give colorless crystals, mp 162 °C; yield: 140 mg (39 %). – IR (KBr): ν = 1715 (s), 1540 (m), 1355 (m), 1235 (vs), 1110 (s), 1090 (s), 1060 (m) cm^{-1}. – ^1H NMR: Tables 1 and 2. – ^{13}C NMR: Table 3. – Anal. calcd. for $C_{29}H_{33}NO_5$ (475.6): C, 73.24; H, 6.99; N, 2.95. Found: C, 72.9; H, 7.0; N, 3.0.

Di(*tert*-butyl) *rel*-(10*S*,10a*S*)-10-(*tert*-butyl)-6,10-diphenyl-3,4,10,10a-tetrahydro-1*H*-[1,4]oxazino[4,3-*a*]azepine-7,8-dicarboxylate (9): A magnetically stirred mixture of allene **4c**[1] (750 mg, 2.25 mmol) and of di(*tert*-butyl) acetylenedicarboxylate (570 mg, 5.04 mmol) was slowly heated to 100 °C until the alkyne melted and a homogeneous solution formed. The reaction mixture was then kept at 100 °C for 14 days, excess alkyne was removed in vacuo by bulb-to-bulb distillation, and the product was isolated by crystallization from acetonitrile at -30 °C. Recrystallization from pentane furnished **9** as a colorless powder, mp 150 °C; yield: 330 mg (26 %). – IR (KBr): ν = 1711 (s), 1655 (s), 1570 (m), 1485 (m), 1445 (m), 1425 (m), 1385 (m), 1360 (s), 1340 (s), 1255 (s), 1245 (s), 1160 (s), 1145 (s), 1100 (m), 1090 (m), 1070 (m), 1015 (m) cm^{-1}. – ^1H NMR: Tables 1 and 2. – ^{13}C NMR: Table 3. – Anal. calcd. for $C_{35}H_{45}NO_5$ (559.8): C, 75.10; H, 8.10; N, 2.50. Found: C, 75.2; H, 8.1; N, 2.6.

X-Ray Crystal Structure Analysis of (E)-7a [14,15]

Crystal Data: $C_{27}H_{27}NO_5$, f. w. 445.5, triclinic, space group $P\bar{1}$; a = 8.339(6), b = 11.126(4), c = 13.591(5) Å; α = 104.03(3), β = 90.03(4), γ = 109.01(4) °; V = 1152.3(22) $Å^3$, Z = 2, D_x = 1.284 $g\,cm^{-3}$; μ(Mo-K_α) = 0.826 cm^{-1}, crystal size 0.6 x 0.4 x 0.2 mm. - *Data collection*: T = 296 K, diffractometer Enraf-Nonius CAD4, monochromatized Mo-K_α radiation, ω/2Θ scans, scan width (1.20 + 0.35 tan Θ) deg, 3363 reflections measured in the range 2.0 ≤ θ ≤ 23.00 deg, 3202 unique reflections (R_{int} = 0.02). - *Structure solution and refinement*: The structure was solved by direct methods and refined by a full-matrix least-squares method based on F values. Hydrogen atoms were included at calculated positions and were treated by a riding model. Refinement with

2559 reflections ($I > 2.5\ \sigma(I)$) and 379 parameters converged at $R = 0.075$, $R_w = 0.088$ (unit weights); the residual electron density was ≤ 0.27 e Å^{-3}.

X-Ray Crystal Structure Analysis of ***8aA*** [14,15]

Crystal Data: $C_{27}H_{27}NO_5$, f. w. 445.5, triclinic, space group $P\bar{1}$; $a = 9.095(5)$, $b = 9.342(5)$, $c = 14.516(8)$ Å; $\alpha = 78.08(4)$, $\beta = 81.16(3)$, $\gamma = 74.20(5)$ °; $V = 1154.9(8)$ Å^3, $Z = 2$, $D_x = 1.281$ g·cm^{-3}; μ(Mo-K$_\alpha$) = 0.82 cm^{-1}, crystal size 0.50 x 0.35 x 0.70 mm. - *Data collection*: $T = 295$ K, diffractometer Enraf-Nonius CAD4, monochromatized Mo-K$_\alpha$ radiation, $\omega/2\Theta$ scans, scan width (0.90 + 0.35 tan Θ) deg, 3784 reflections measured in the range $2.0 \le \theta \le 24.00$ deg, 3620 unique reflections ($R_{int} = 0.074$); a correction for intensity loss (up to 0.9 %) was applied. - *Structure solution and refinement*: The structure was solved by direct methods (program SIR) and refined by a full-matrix least-squares method based on F values. Most hydrogen atom positions were located in a ΔF map and refined with isotropic temperature factors, H17A-C and H19A were included at calculated positions and were not refined. Refinement with 2530 reflections ($I > 2.5\ \sigma(I)$) and 390 parameters converged at $R = 0.0737$, $R_w = 0.0875$ ($w = [\sigma(F_o^2) + (0.025\ F_o)^2]^{-1}$); the residual electron density was ≤ 0.28 e Å^{-3}.

X-Ray Crystal Structure Analysis of ***8c*** [14,15]

Crystal Data: $C_{29}H_{33}NO_5$, f. w. 475.6, orthorhombic, space group $P2_12_12_1$; $a = 10.393(3)$, $b = 13.288(3)$, $c = 18.023(3)$ Å; $\alpha = 90$, $\beta = 90$, $\gamma = 90$ °; $V = 2489.1(9)$ Å^3, $Z = 4$, $D_x = 1.269$ g·cm^{-3}; μ(Mo-K$_\alpha$) = 0.81 cm^{-1}, crystal size 0.75 x 0.50 x 0.45 mm. - *Data collection*: $T = 295$ K, diffractometer Enraf-Nonius CAD4, monochromatized Mo-K$_\alpha$ radiation, $\omega/2\Theta$ scans, scan width (0.95 + 0.35 tan Θ) deg, 2839 reflections measured in the range $2.0 \le \theta \le 25.00$ deg, 2732 unique reflections ($R_{int} = 0.039$). - *Structure solution and refinement*: The structure was solved by direct methods (program SIR) and refined by a full-matrix least-squares method based on F values. All hydrogen atom positions were located in a ΔF map and refined with isotropic temperature factors, except for H14 and H19A-C which were treated by a riding model. Refinement with 2143 reflections ($I > 2\ \sigma(I)$) and 403 parameters converged at $R = 0.0458$, $R_w = 0.0408$ ($w = [\sigma(F_o^2) + (0.018\ F_o)^2]^{-1}$); the residual electron density was ≤ 0.21 e Å^{-3}. The absolute structure was not determined.

Acknowledgement

This work was supported by the Deutsche Forschungsgemeinschaft and the Fonds der Chemischen Industrie.

References and Notes

[1] (a) Maas, G.; Mayer, T. *Synlett* **1990**, 399-400. (b) Maas, G.; Mayer, T. *Synthesis* **1991**, 1209-1215.
[2] Maas, G.; Reinhard, R.; Neumann, R.; Glaser, M. *J. prakt. Chem.* **1996**, *338*, 441-450.
[3] Klop, W.; Klusener, P. A. A.; Brandsma, L. *Recl. Trav. Chim. Pays-Bas* **1984**, *103*, 85-86.
[4] Brandsma, L.; Klop, W. *J. Chem. Soc., Chem. Commun.* **1983**, 988-989.
[5] Maas, G.; Mayer, T. *Tetrahedron Lett.* **1992**, *33*, 205-208.
[6] Reinhard, R.; Glaser, M.; Neumann, R.; Maas, G. *J. Org. Chem.* **1997**, *62*, 7744-7751.
[7] For 1,7-electrocyclic reactions of other α,ß,γ,δ-unsaturated 1,3-dipoles, see: Zecchi, G. *Synthesis* **1991**, 181-188.
[8] Verboom, W.; Reinhoudt, D. W. *Recl. Trav. Chim. Pays-Bas* **1990**, *109*, 311-324.
[9] Meth-Cohn, O., *Adv. Heterocyclic Chem.* **1996**, *65*, 1-36.
[10] (a) De Boeck, B.; Jiang, S.; Janousek, Z.; Viehe, H. G. *Tetrahedron* **1994**, *50*, 7075-7092. (b) De Boeck, B.; Viehe, H. G. *Tetrahedron* **1998**, *54*, 513-520.

[11] Crabb, T. A.; Roch, O. G. *J. Chem. Soc., Perkin Trans. 2* **1992**, 949-953. (b) Jupp, P. A.; Crabb, T. A. *J. Chem. Soc., Perkin Trans. 1*, **1985**, 913-918. (c) Jupp, P. A.; Crabb, T. A. *J. Chem. Soc. Perkin Trans. 2*, **1980**, 1778-1782.

[12] Meise, W.; Zlotos, D.; Jansen, M.; Zoche, N. *Liebigs Ann. Chem.* **1995**, 567-574. Zlotos, D. P.; Meise, W. *Heterocycles* **1997**, *45*, 2137-2157.

[13] Roxburgh, C. J. *Tetrahedron* **1994**, *50*, 13199-13206.

[14] All calculations were done with the program package *MolEN, An Interactive Structure Solution Procedure* (Enraf-Nonius, Delft, The Netherlands, 1990). Molecule plots were made with *PLUTON-92* (A. Spek, University of Utrecht, **1992**).

[15] Crystallographic data (excluding structure factors) for the X-ray crystal structure analyses reported in this paper have been deposited with the Cambridge Crystallographic Data Centre. Copies of the data can be obtained free of charge on application to CCDC, 12 Union Road, Cambridge CB2 1EZ, UK (fax: int. code +(1223) 336-033, e-mail: deposit@ccdc.cam.ac.uk).